

Contribution from the Department of Chemistry and Biochemistry, University of Notre Dame, Notre Dame, Indiana 46556, and Department of Chemistry, Princeton University, Princeton, New Jersey 08544

Influence of Porphyrin Radical Type on V=O Bond Strength in Vanadyl Porphyrin Cation Radicals: Implications for Heme Protein Intermediates

Kathleen A. Macor,^{*†} Roman S. Czernuszewicz,^{‡§} and Thomas G. Spiro[†]

Received August 18, 1989

Resonance Raman spectra have been analyzed for vanadyl porphyrin cation radicals of octaethylporphyrin (OEP), *meso*-tetraphenylporphyrin (TPP), and *meso*-tetramesitylporphyrin (TMP). The strength of the metal–oxo bond in these cation radicals is demonstrated to be a function of radical type, “a_{1u}” or “a_{2u}”. Porphyrin ring mode ν_2 , which has previously been shown to be a marker for the radical type, was used to identify the radicals. The a_{1u} OV(OEP) radical exhibited an upshift in the V=O stretching frequency resulting from the increased positive charge on the porphyrin, which reduces the porphyrin \rightarrow vanadium electron donation and increases the O \rightarrow vanadium donation. $\nu(\text{V}=\text{O})$ frequency decreases were observed for the a_{2u} OV(TPP) and OV(TMP) radicals. These can be explained on the basis of mixing of the porphyrin π a_{2u} orbital with the vanadium d_z and oxygen p_z orbitals, which is allowed in C_{4v} symmetry. This interaction decreases the bond strength in a_{2u} cation radicals, since an electron is removed from an orbital with partial V–O σ -bonding character. Mixing of the porphyrin a_{1u} π orbital with metal or oxygen orbitals is forbidden. These results imply that porphyrin radical type is an important determinant of the Fe=O bond strength in heme protein cation-radical intermediates.

Introduction

Porphyrins that contain metal–oxo bonds have been extensively studied as models for the heme protein active sites of the peroxidases, catalases, and cytochrome P₄₅₀'s. Catalases decompose hydrogen peroxide to oxygen and water, whereas peroxidases oxidize organic and inorganic substrates via reaction with peroxides and other oxidants. The active sites of both enzymes, known as compound I, are porphyrin cation radicals that contain ferryl (Fe=O) bonds. Cytochrome P₄₅₀, which hydroxylates a variety of organic molecules via an oxygen atom transfer mechanism, reduces molecular oxygen to generate a ferryl intermediate of the same formal oxidation state as compound I. The catalytic cycles of these enzymes have been extensively reviewed.¹

There is considerable interest in utilizing metal–oxo porphyrins as catalysts for oxidative reactions, ranging from hydrocarbon oxidation to water splitting.² Manganese, chromium, and iron porphyrins react with oxygen atom transfer reagents, such as iodobenzene, *m*-chloroperoxybenzoic acid, and sodium hypochlorite, yielding Mn^{VO}₃ and Cr^{VO}₄ porphyrins and Fe^{IVO} porphyrin cation radicals.⁵ These are potent oxidizing agents that are capable of catalytic oxygen atom insertion into hydrocarbons. Fe^{IVO} porphyrins have been generated via low-temperature decomposition of peroxy-bridged intermediates⁶ and irradiation of PFe^{II}O₂ adducts at 12 K in argon matrices.⁷ Electrochemical oxidation in hydroxide-containing solutions has produced both Fe^{IVO} and Mn^{IVO}₃ porphyrins. Resonance Raman spectroscopy has been extensively used to characterize the metal–oxo bonds in ferryl porphyrins^{7,8a,10} and proteins,¹¹ and the Mn^{IV}=O Raman stretch was recently observed.⁹

Vanadyl porphyrins contain a stable V–O bond and provide a convenient model system for the more reactive ferryl porphyrins. H-bonding and axial ligand interactions have been monitored for V=O porphyrins with resonance Raman spectroscopy.¹² The vanadyl porphyrin cation radical has also been studied,¹² and the V–O stretching frequency was reported to increase 15 cm⁻¹ in OV(OEP)^{•+} (OEP = octaethylporphyrin).

In the present study we have observed that the direction of the cation-radical shift of the metal–oxo bond frequency is dependent on the spin density pattern of the cation radical. Porphyrin ring mode ν_2 , which has previously been shown to be marker for radical type,¹³ was used to identify the radicals. An upshift of this mode indicates an a_{1u} radical, while a downshift is characteristic of an a_{2u} radical. The shift directions have been explained on the basis

of electron removal from antibonding and bonding orbitals, respectively. The a_{1u} OV(OEP) radical exhibits an upshift in the

- (1) (a) Ortiz de Montellano, P. R. *Acc. Chem. Res.* **1987**, *20*, 289–294. (b) Ortiz de Montellano, P. R., Ed. *Cytochrome P450 Structure, Mechanism, and Biochemistry*; Plenum: New York, 1986. (c) Guengerich, F. P.; MacDonald, T. L. *Acc. Chem. Res.* **1984**, *17*, 9–16. (d) Hewson, W. D.; Hager, L. P. In *The Porphyrins*; Dolphin, D., Ed.; Academic Press: New York, 1979; Vol. 7, Chapter 6. (e) Dunford, H. B.; Stillman, J. S. *Coord. Chem. Rev.* **1976**, *19*, 187–251.
- (2) (a) Creager, S. E.; Raybuck, S. A.; Murray, R. W. *J. Am. Chem. Soc.* **1986**, *108*, 4225–4227. (b) Collman, J. P.; Brauman, J. I.; Meunier, B.; Hayashi, T.; Kodadek, T.; Raybuck, S. A. *J. Am. Chem. Soc.* **1985**, *107*, 2000–2005. (c) Powell, M. F.; Pai, E.; Bruce, T. C. *J. Am. Chem. Soc.* **1984**, *106*, 3277–3285. (d) Harriman, A.; Porter, G.; Walters, P. *J. Chem. Soc., Faraday Trans. 1* **1983**, *79*, 1335–1350.
- (3) (a) Schappacher, M.; Weiss, R. *Inorg. Chem.* **1987**, *26*, 1190–1192. (b) Groves, J. T.; Stern, M. K. *J. Am. Chem. Soc.* **1987**, *109*, 3812–3814. (c) Bortoloni, O.; Meunier, B.; Friant, P.; Ascone, I.; Goulon, J. *Nouv. J. Chim.* **1986**, *10*, 39–49.
- (4) (a) Penner-Hahn, J. E.; Benfatto, M.; Hedman, B.; Takahashi, T.; Sebastian, D.; Groves, J. T.; Hodgson, K. O. *Inorg. Chem.* **1986**, *25*, 2255–2259. (b) Groves, J. T.; Kruper, W. J. *J. Am. Chem. Soc.* **1979**, *101*, 7613–7615.
- (5) (a) Balch, A. L.; La Mar, G. N.; Latos-Grazynsky, L.; Renner, M. W.; Thanabal, V. *J. Am. Chem. Soc.* **1985**, *107*, 3003–3007. (b) Groves, J. T.; Haushalter, R. C.; Nakamura, M.; Nemo, T. E.; Evans, B. J. *J. Am. Chem. Soc.* **1981**, *103*, 2884–2886.
- (6) Chin, D. H.; La Mar, G. N.; Balch, A. L. *J. Am. Chem. Soc.* **1980**, *102*, 5945–5946.
- (7) (a) Proniewicz, L. M.; Bajdor, K.; Nakamoto, K. *J. Phys. Chem.* **1986**, *90*, 1760–1766. (b) Bajdor, K.; Nakamoto, K. *J. Am. Chem. Soc.* **1984**, *106*, 3045–3046.
- (8) (a) Czernuszewicz, R. S.; Macor, K. A. *J. Raman Spectrosc.* **1988**, *19*, 553–557. (b) Groves, J. T.; Gilbert, J. A. *Inorg. Chem.* **1986**, *25*, 123–125. (c) Lee, W.; Calderwood, T. S.; Bruce, T. C. *Proc. Natl. Acad. Sci. U.S.A.* **1985**, *82*, 4301–4305. (d) Calderwood, T. S.; Lee, W. A.; Bruce, T. C. *J. Am. Chem. Soc.* **1985**, *107*, 8272–8273.
- (9) Czernuszewicz, R. S.; Su, Y. O.; Stern, M. K.; Macor, K. A.; Kim, D.; Groves, J. T.; Spiro, T. G. *J. Am. Chem. Soc.* **1988**, *110*, 4158–4165.
- (10) (a) Kincaid, J. R.; Schneider, A. J.; Paeng, K. J. *J. Am. Chem. Soc.* **1989**, *111*, 735–737. (b) Paeng, I. R.; Shiwaku, H.; Nakamoto, K. *J. Am. Chem. Soc.* **1988**, *110*, 1995–1996. (c) Hashimoto, S.; Tatsuno, Y.; Kitagawa, T. *J. Am. Chem. Soc.* **1987**, *109*, 8096–8097. (d) Kean, R. T.; Oertling, W. A.; Babcock, G. T. *J. Am. Chem. Soc.* **1987**, *109*, 2185–2187. (e) Schappacher, M.; Chottard, G.; Weiss, R. *J. Chem. Soc. Chem. Commun.* **1986**, 93–94. (f) Hashimoto, S.; Tatsuno, Y.; Kitagawa, T. In *Proceedings of the Tenth International Conference on Raman Spectroscopy*; University of Oregon Press: Eugene, OR, 1986; p 1-28.
- (11) (a) Paeng, K. J.; Kincaid, J. R. *J. Am. Chem. Soc.* **1988**, *110*, 7913–7915. (b) Ogura, T.; Kitagawa, T. *J. Am. Chem. Soc.* **1987**, *109*, 2177–2179. (c) Hashimoto, S.; Tatsuno, Y.; Kitagawa, T. *Proc. Natl. Acad. U.S.A.* **1986**, *83*, 2417–2421. (d) Terner, J.; Sitter, A. J.; Reczek, C. M. *Biochim. Biophys. Acta* **1985**, *828*, 73–80. (e) Oertling, W. A.; Babcock, G. T. *J. Am. Chem. Soc.* **1985**, *107*, 6406–6407. (f) Van Wart, H. E.; Zimmer, J. *J. Am. Chem. Soc.* **1985**, *107*, 3379–3381.
- (12) Su, Y. O.; Czernuszewicz, R. S.; Miller, L. A.; Spiro, T. G. *J. Am. Chem. Soc.* **1988**, *110*, 4150–4157.
- (13) Czernuszewicz, R. S.; Macor, K. A.; Li, X. Y.; Kincaid, J. R.; Spiro, T. G. *J. Am. Chem. Soc.* **1989**, *111*, 3860–3869.

* To whom correspondence should be addressed.

[†] University of Notre Dame.

[‡] Princeton University.

[§] Present address: Department of Chemistry, University of Houston, Houston, TX 77004.

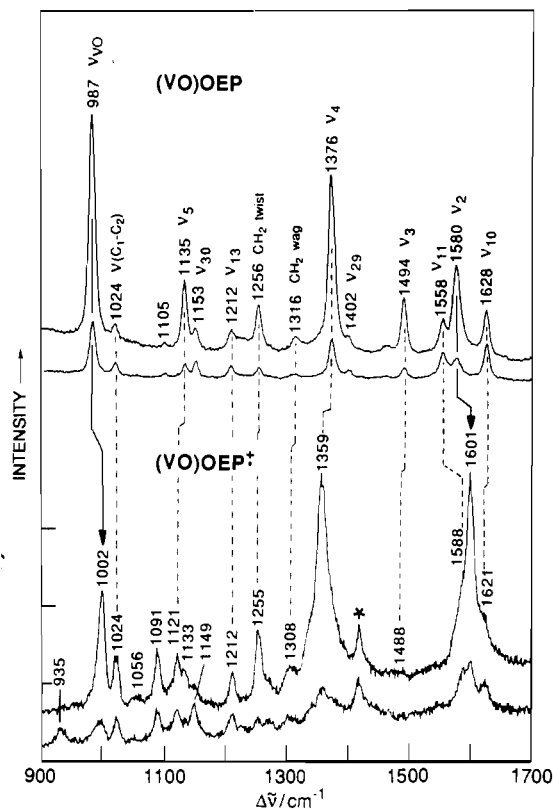


Figure 1. Resonance Raman spectra of OV(OEP) and OV(OEP)⁺⁺ in parallel (||) and perpendicular (⊥) polarizations obtained with 406.7-nm excitation. Conditions: 50-mW laser power and 8-cm⁻¹ slit widths. Asterisks indicate CH₂Cl₂ solvent bands, and arrows indicate the upshifts of $\nu(\text{V}=\text{O})$ and ν_2 modes upon cation-radical formation.

$\text{V}=\text{O}$ stretching frequency from the increased positive charge on the porphyrin, which reduces the porphyrin \rightarrow vanadium electron donation and increases the $\text{O} \rightarrow$ vanadium donation. $\nu(\text{V}=\text{O})$ frequency decreases were observed for the a_{2u} OV(TPP) (TPP = tetraphenylporphyrin) and OV(TMP) (TMP = tetramesitylporphyrin) radicals. These can be explained on the basis of mixing of the porphyrin πa_{2u} with the vanadium d_{2z} and oxygen p_z orbitals, which is allowed in C_{4v} symmetry. This interaction decreases the bond strength in a_{2u} cation radicals, since an electron is removed from an orbital with partial $\text{V}-\text{O}$ σ -bonding character. Mixing of the porphyrin a_{1u} π orbital with metal or oxygen orbitals is forbidden.

These results imply that porphyrin radical type is an important determinant of the $\text{Fe}=\text{O}$ bond strength in heme protein cation-radical intermediates.

Experimental Section

Chemicals. Vanadyl octaethyl-, *meso*-tetraphenyl-, and *meso*-tetramesitylporphyrins were obtained from Mid-Century Chemicals (Posen, IL) and were purified on thin-layer alumina plates. Tetrabutylammonium perchlorate (TBAP) (GFS Chemicals, Columbus, OH) was recrystallized from ethyl acetate and dried under vacuum at 90 °C. CH₂Cl₂ was distilled over CaH₂ prior to use. The ¹⁸O-vanadyl isomers were prepared from the dichlorovanadium(IV) porphyrins, which were supplied by Mid-Century Chemicals, by treatment with H₂¹⁸O (Cambridge Isotopes, Boston, MA).

Oxidations. Vanadyl porphyrin cation radicals were prepared by controlled-potential electrolysis of the oxovanadium(IV) porphyrins in 0.1 M TBAP/CH₂Cl₂ with a Princeton Applied Research 173 potentiostat, 175 programmer, and 179 coulometer. The three-electrode Raman spectroelectrochemical cell was described previously.^{8a} A Pt anode and saturated calomel reference electrode were used. The oxidations were carried at room temperature and -80 °C for OV(OEP) and OV(TPP), respectively. A small amount of irreversible porphyrin decomposition was observed when OV(TPP) was oxidized at room temperature; at low temperature oxidation was reversible, however. The course of electrooxidation was followed by monitoring porphyrin Raman band ν_2 , since the position of this band is sensitive to porphyrin ring oxidation. Following oxidation and cation radical data acquisition, the solutions

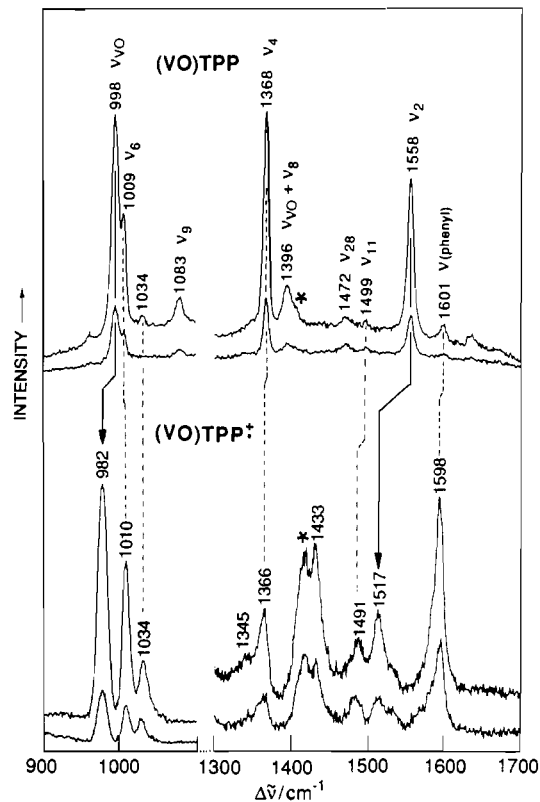


Figure 2. Resonance Raman spectra of OV(TPP) and OV(TPP)⁺⁺ in parallel (||) and perpendicular (⊥) polarizations obtained with 406.7- (900–1100 cm⁻¹) and 457.9-nm (1300–1700 cm⁻¹) excitation. Conditions are as in Figure 1. Asterisks indicate CH₂Cl₂ solvent bands, and arrows indicate the downshifts of $\nu(\text{V}=\text{O})$ and ν_2 modes upon cation-radical formation.

were reduced at 0.2 V. In each case the neutral species spectrum was recovered.

Raman Measurements. Resonance Raman spectra were obtained in backscattering geometry from porphyrin solutions by using the Raman spectroelectrochemical cell^{8a} previously described. Exciting radiation was provided by Coherent Radiation Innova 100K-3 krypton and Spectra Physics Model 2025 argon ion lasers. The scattered radiation was dispersed by a Spex 1401 double monochromator and detected by a cooled RCA 31034A photomultiplier tube using an Ortec 9315 photon-counting system, under the control of an IBM XT computer.

Results

The high frequency region resonance Raman (RR) spectra shown in Figures 1 and 2 identify the OV(OEP) and OV(TPP) radicals as a_{1u} and a_{2u} , respectively, on the basis of the shift directions of porphyrin ring mode ν_2 upon cation-radical formation. It has previously been shown from a study of metalated OEP and TPP radicals¹³ that mode ν_2 is an indicator of radical type, shifting down 25–40 cm⁻¹ for a_{2u} radicals and displaying 20–25 cm⁻¹ upshifts for a_{1u} radicals. ν_2 is composed of mainly pyrrole $C_\beta C_\beta$ stretching. The $C_\beta C_\beta$ interaction is bonding and antibonding, in the a_{2u} and a_{1u} orbitals, respectively (see Figure 4a). Removing an electron from the former orbital results in a weaker bond with a lower stretching frequency, whereas a higher stretching frequency is observed for the latter, since the electron is removed from an antibonding orbital. Band ν_2 is seen at 1580 cm⁻¹ in OV(OEP). If shifts up 21 cm⁻¹ to 1601 cm⁻¹ in OV(OEP)⁺⁺ (Figure 1), whereas a 41-cm⁻¹ downshift is observed from 1558 cm⁻¹ in OV(TPP) to 1517 cm⁻¹ in OV(TPP)⁺⁺ (Figure 2). A downshift of 40 cm⁻¹ was also seen for OV(TMP)⁺⁺, whose spectrum (not shown) is similar to that of OV(TPP)⁺⁺.

The strong band at 1598 cm⁻¹ in the spectrum of OV(TPP)⁺⁺ (Figure 2) is phenyl mode ν_{8a} , which appears at 1601 cm⁻¹ in OV(TPP). Phenyl mode intensity increases are characteristic of porphyrin cation radicals¹³ and may result from a tilt of the phenyl rings toward planarity with the porphyrin ring, which has been observed in cation radical X-ray crystal structures.¹⁴

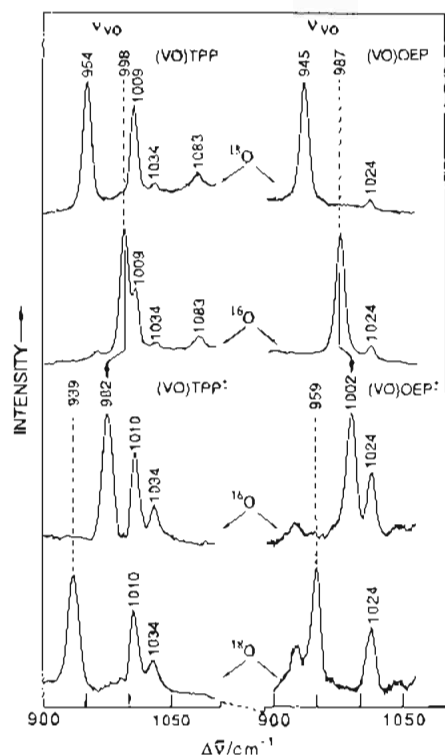


Figure 3. Resonance Raman spectra of OV(TPP) and OV(TPP)^{+•} (left panel) and OV(OEP) and OV(OEP)^{+•} (right panel) and their ¹⁸O-isotopomers obtained with 406.7-nm excitation. Conditions are as in Figure 1. The arrows indicate shifts of $\nu(\text{V}=\text{}^{16}\text{O})$ upon cation-radical formation.

The metal-oxo bond strength decreases upon formation of the a_{2u} OV(TPP) radical, whereas the opposite effect occurs in the a_{1u} OV(OEP) radical. The $\text{V}=\text{O}$ stretch seen at 987 cm^{-1} in the OV(OEP) spectrum in Figure 1 shifts up 15 cm^{-1} to 1002 cm^{-1} in the radical. In contrast, this band observed at 998 cm^{-1} in OV(TPP) exhibits a 16-cm^{-1} downshift to 982 cm^{-1} in OV(TPP)^{+•} (Figure 2). A downshift of 14 cm^{-1} was also observed for OV(TMP)^{+•}. The $\text{V}=\text{O}$ stretching bands were identified by the 43-cm^{-1} downshifts observed for the unoxidized and cation-radical porphyrins containing ¹⁸O-labels. $\nu(\text{V}=\text{}^{18}\text{O})$ is observed at 959 and 939 cm^{-1} in the ¹⁸O adducts of OV(OEP)^{+•} and OV(TPP)^{+•}, respectively, as seen in Figure 3.

The $\text{V}=\text{O}$ stretching mode is one of the strongest bands in the Soret-excited resonance Raman spectra. The Soret transition populates the set of lowest unoccupied porphyrin orbitals (e_g^*), which are mixed with the antibonding $d_{xz}-\text{O } p_x$ and $d_{yz}-\text{O } p_y$ orbitals (e_g^*) (see Figure 5). Metal-ligand modes are enhanced to the extent that the metal-ligand bond lengths are altered in the resonant excited state.¹⁵ Population of the e_g^* orbital in the excited state lengthens the $\text{V}-\text{O}$ bond due to competition with the oxygen π electrons for the empty d_x vanadium orbitals. The relative intensities indicate that the $\text{V}-\text{O}$ bond lengthening is comparable to the alteration of the porphyrin ring bonds in the excited state.

Discussion

1. Mechanisms for $\nu(\text{V}=\text{O})$ Frequency Change in Cation Radicals. A. Polarization Effect. The metal-oxo bond strength increases upon formation of the a_{1u} OV(OEP) radical. The $\text{V}=\text{O}$ stretch seen at 987 cm^{-1} in the OV(OEP) spectrum in Figure 1 shifts up 15 cm^{-1} to 1002 cm^{-1} in the radical. An increase in frequency is expected on the basis of bond polarization; the one-electron deficient porphyrin radical cation donates less electron density to vanadium, resulting in increased $\text{O} \rightarrow \text{V}$ donation and

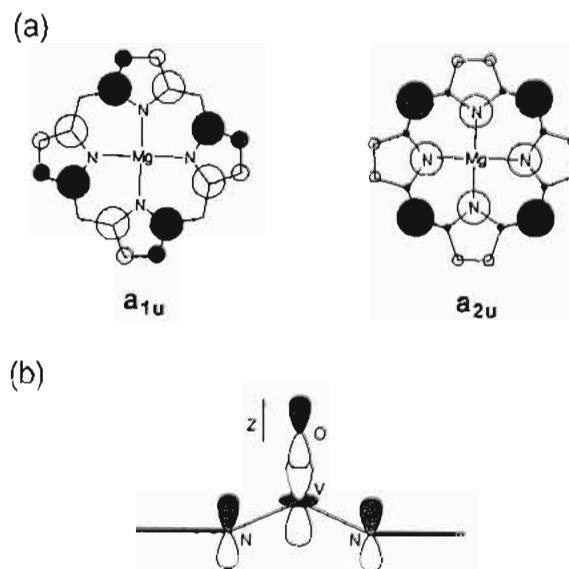


Figure 4. (a) Atomic orbital (AO) structure of magnesium porphyrin in the two highest occupied molecular orbitals, a_{1u} and a_{2u} . The circle sizes are approximately proportional to the AO coefficients.¹³ The open circles represent negative signs of the upper lobe of the p_x AO's. (b) Illustration of the porphyrin a_{2u} , vanadium d_{2z} , and oxygen p_z σ -bonding interaction, which is responsible for the $\nu(\text{V}=\text{O})$ downshift in a_{2u} porphyrin cation radicals. (Only two porphyrin nitrogens are shown.) The shaded circles represent negative signs of the orbitals.

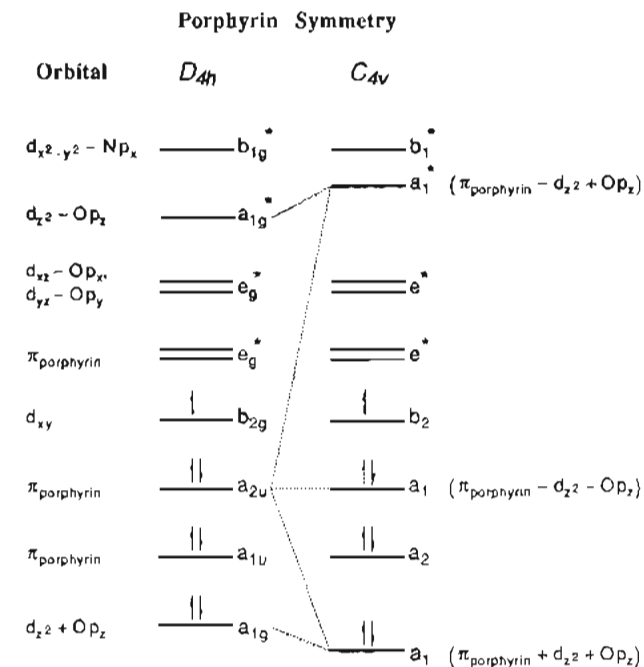


Figure 5. Qualitative D_{4h} and C_{4v} orbital energy level diagram, which illustrates the mixing between the porphyrin a_{2u} , metal d_{z^2} , and oxygen p_z orbitals in C_{4v} symmetry. Mixing of the porphyrin a_{1u} orbital with metal or oxygen orbitals is forbidden. In D_{4h} symmetry, no interactions are possible between the a_{2u} or a_{1u} HOMO's and any metal orbitals (all of which are "g").

a stronger $\text{V}=\text{O}$ bond. The magnitude of the shift is comparable to the difference in $\nu(\text{V}=\text{O})$ between OV(TMPyP) (TMPyP = tetrakis(methylpyridinium)porphyrin) and OV(TPP), 17 cm^{-1} (in nonacceptor solvents).¹² OV(TMPyP) has four positive charges on the four peripheral pyridyl groups. It seems reasonable that their inductive effect is about the same as that of a single positive charge on the porphyrin ring itself. The inductive effect should be even larger for an a_{2u} than an a_{1u} radical, since the former concentrates charge on the pyrrole N atoms, which are bonded to the vanadium, whereas the a_{1u} orbital has nodes at the N atoms. Consequently, the downshift associated with radical formation

(14) Scheidt, W. R.; Lee, Y. J. *Struct. Bonding* 1987, 64, 1-70 and references therein.

(15) Spiro, T. G. In *Iron Porphyrins*; Lever, A. B. P., Gray, H. B., Eds.; Addison-Wesley: Reading, MA, 1983; Part II, pp 89-159.

in OV(TPP) and OV(TMP) requires an additional mechanism.

B. Steric Factors. The possibility needs to be considered that the altered peripheral substituents are themselves responsible for bonding differences between OV(OEP)^{•+} and OV(TPP)^{•+} and OV(TMP)^{•+}. We note that TPP cation radicals frequently display saddle-shaped structures¹⁴ in which the phenyl rings are rotated significantly toward the porphyrin plane and the pyrrole rings are displaced alternately up and down. This concerted distortion might be an intrinsic electronic effect, since the a_{2u} radicals concentrate charge on the methine bridges (as well as the porphyrin N atoms) and this charge could be delocalized onto the phenyl π systems to the extent that the phenyl and porphyrin π orbitals approach coplanarity. If the saddle distortion is intrinsic and is specific to TPP, it might explain the V–O frequency decrease because there would be increased nonbonded repulsion between two pyrrole N atoms (the two upwardly displaced pyrroles) and the vanadyl O atom.

However, Scheidt¹⁴ has argued that the tilt of the phenyl rings is an intermolecular effect, since it allows a close approach of two porphyrin rings. All the saddle-distorted TPP radical structures do show dimer formation in the solid. Supporting this view is the recent finding that Cu(TMP)^{•+} is monomeric in the solid state,¹⁶ the bulky mesityl groups presumably inhibiting dimer formation, and the porphyrin ring is planar. Since we find the same ν(V=O) downshift for OV(TMP)^{•+} as for OV(TPP)^{•+}, it seems very unlikely that the effect can be attributed to steric factors.

C. HOMO Differences. We offer an explanation for the V=O bond weakening in a_{2u} radicals based on orbital mixing, which becomes permitted upon symmetry reduction from D_{4h} to C_{4v}. Figure 5 provides a qualitative D_{4h} and C_{4v} orbital energy level diagram. The highest occupied orbital (HOMO) of a D_{4h} metalloporphyrin is a_{1u} or a_{2u} depending upon a combination of factors including porphyrin ring substituents and axial ligands.¹⁷ The O²⁻ ligand donates σ and π electrons to the V⁴⁺ ion. The filled p_x orbitals on the ligand (p_x and p_y, with z as the M–O direction) interact with the d_{xz} orbitals (d_{xz}, d_{yz}), which become antibonding. The d_{z²} and d_{x²-y²} orbitals are σ antibonding with respect to the V–O bond and the V–N bonds, respectively, and are at higher energy. The d_{xy} orbital is nonbonding. This orbital accommodates the single d electron of V⁴⁺, allowing unimpeded O → M π interactions. Since there are two π orbital overlaps, the result is formally a M=O triple bond. EPR spectroscopy¹⁸ indicates that there is one unpaired electron on the vanadium in a relatively pure d_{xy} orbital in the unoxidized porphyrin and that one-electron oxidation removes an electron from a porphyrin orbital.

In D_{4h} symmetry, no interactions are possible between the porphyrin a_{2u} or a_{1u} HOMO's and any metal orbitals (all of which are "g"). When the symmetry is C_{4v}, however, the a_{2u} and d_{z²} orbitals both become a₁. Orbital overlap becomes possible because the V atom is displaced (by 0.5 Å¹⁹) from the porphyrin plane. Because the d_{z²} orbital interacts strongly with the oxygen p_z orbital, three orbitals are produced by the a_{2u} interaction. The orbital of lowest energy (Figure 5) is completely bonding (zero nodes) and contains two electrons. The highest energy orbital has two nodes and is antibonding with respect to both the porphyrin–vanadium and the vanadium–oxygen interactions. This orbital is unoccupied. The middle energy orbital, which is the HOMO, contains one node and is, to first-order, σ nonbonding with respect to the V–N and V–O bonds. However, orbital mixing imparts a small amount of d_{z²} + O p_z character to the HOMO. Figure 4b illustrates the V–O–porphyrin bonding interaction. Consequently, removing an electron partially weakens the O–V σ bond

and can account for the ~15-cm⁻¹ downshift observed for the "a_{2u}" OV(TPP)^{•+} and OV(TMP)^{•+} radicals. This mechanism is unavailable to OV(OEP)^{•+}, since the a_{1u} orbital (a₂ in C_{4v} symmetry) remains unable to mix with the vanadium orbitals.

EPR spectra of halide-ligated Zn and Co(TPP) cation radicals exhibit metal and axial ligand hyperfine splitting.²⁰ Such splitting is observed along with nitrogen hyperfine splitting, which designates the radicals as a_{2u}, since electron density is mainly localized on the nitrogens and meso carbons in these radicals. These results clearly indicate that in a_{2u} radicals spin density is transmitted to axial ligands via the nitrogens. In contrast, a_{1u} radicals have little, if any, spin density on the nitrogens and are without a mechanism to deliver spin density to axial ligands. Charge-iterative extended Hückel calculations on ferryl porphyrins have also indicated that a small amount of spin density resides on the oxo ligand in a_{2u}, but not a_{1u}, radicals.²¹

2. Implications for Heme Proteins. Recently, a 41-cm⁻¹ downshift of ν(Fe=O) along with a ~40-cm⁻¹ downshift for porphyrin mode ν₂ was reported for OFe(TMP)^{•+}^{10a} generated by *m*-chloroperoxybenzoic acid oxidation of Fe(TMP)Cl in toluene at -80 °C. The ferryl TMP adduct was prepared by cleavage of the peroxy-bridged species also in toluene.^{10b,f} The ν₂ shift indicates that OFe(TMP)^{•+} is an a_{2u} radical, as expected, and the downshift of ν(Fe=O) is in accord with the orbital-mixing mechanism. The fact that the shift is substantially larger than that seen for OV(TMP)^{•+} (41 vs 14 cm⁻¹) suggests that the orbital mixing is also greater for OFe(TMP)^{•+}. This can be understood on the basis of a better energy match between the a_{2u} orbital and the Fe d_{z²} + O p_z orbital, due to the weaker Fe–O bond. Fe(IV) has three more electrons than V(IV), and the Fe d_{x²-y²} – O p_x e_g^{*} orbitals (Figure 5) each contain one electron. Consequently the M–O bond order is reduced to two,⁹ and ν(Fe=O), 843 cm⁻¹, is substantially lower than ν(V=O), 991 cm⁻¹. The weaker Fe–O bond implies a smaller σ overlap and consequently a higher energy for the d_{z²} + p_z orbital than for the V–O bond. This energy increase would lead to more extensive mixing with the a_{2u} orbital, thereby increasing the ν(M=O) shift.

The present work has implications for the vibrational structures of oxidative heme proteins. HRP compound I has been inferred to contain an a_{2u} radical ferryl heme, on the basis of EPR,²² Mössbauer,^{22a,23} and ENDOR²⁴ evidence. Although protoporphyrin, like OEP, is expected to produce a_{1u} radicals, the a_{2u} orbital could become the HOMO through the donor effect of the sixth ligand, imidazole, provided by the protein. This inversion would be consistent with the electronic structure calculations^{20a,21} of Hanson et al. Mixing of a_{1u} and a_{2u} orbitals is expected (and calculated²¹) because the very different axial ligands, imidazole and oxo, impose C_{4v} symmetry. If the a_{2u} assignment is correct, then a weakened Fe=O bond would be expected for compound I in relation to compound II, which contains a ferryl neutral porphyrin.^{1d} In a recent resonance Raman study of HRP compound I^{1a} a 39-cm⁻¹ downshift of ν(Fe=O) has, in fact, been reported along with a 15-cm⁻¹ downshift of mode ν₂, the expected direction for an a_{2u} radical. However, another resonance Raman study of compound I²⁵ reports an upshifted ν₂ mode. Assignment of this band is complicated by the presence of multiple bands in the 1550–1650-cm⁻¹ region in both spectra. In addition, different laser excitations (356.4 vs 406.7 nm) were used in the two studies

- (16) Song, H.; Reed, C. A.; Schedit, W. R. *J. Am. Chem. Soc.* **1989**, *111*, 6865–6866.
 (17) Fajer, J.; Borg, D. C.; Forman, A.; Dolphin, D.; Felton, R. H. *J. Am. Chem. Soc.* **1970**, *92*, 3451–3459.
 (18) (a) Lin, W. C. In *The Porphyrins*; Dolphin, D., Ed.; Academic Press: New York, 1979; Vol. 4, Chapter 7. (b) Luckhurst, G. R.; Setaka, M.; Subramanian, J. *Mol. Phys.* **1976**, *32*, 1299–1309. (c) Newton, C. M.; Davis, D. G. *J. Magn. Reson.* **1975**, *20*, 446–457.
 (19) (a) Drew, M. G.; Mitchell, P. C.; Scott, C. E. *Inorg. Chim. Acta* **1984**, *82*, 63–67. (b) Molinaro, F. S.; Ibers, J. A. *Inorg. Chem.* **1976**, *15*, 2278–2282.

- (20) (a) Fujita, I.; Hanson, L. K.; Walker, F. A.; Fajer, J. *J. Am. Chem. Soc.* **1983**, *105*, 3296–3300. (b) Fajer, J.; Davis, M. S. In *The Porphyrins*; Dolphin, D., Ed.; Academic Press: New York, 1979; Vol. 4, Chapter 4. (c) Fajer, J.; Borg, D. C.; Forman, A.; Felton, R. H.; Vegh, L.; Dolphin, D. *Ann. N.Y. Acad. Sci.* **1973**, *206*, 349–364.
 (21) Hanson, L. K.; Chang, C. K.; Davis, M. S.; Fajer, J. *J. Am. Chem. Soc.* **1981**, *103*, 663–670.
 (22) (a) Rutter, R.; Valentine, M.; Hendrich, M. P.; Hager, L. P.; Debrunner, P. G. *Biochemistry* **1983**, *22*, 4769–4774. (b) Roberts, J. E.; Hoffman, B. M.; Rutter, R.; Hager, L. P. *J. Am. Chem. Soc.* **1981**, *103*, 7654–7656.
 (23) Schulz, C. E.; Devaney, P. W.; Winkler, H.; Debrunner, P. G.; Doan, N.; Chiang, R.; Rutter, R.; Hager, L. P. *FEBS Lett.* **1979**, *103*, 102–105.
 (24) Roberts, J. E.; Hoffman, B. M.; Rutter, R.; Hager, L. P. *J. Biol. Chem.* **1981**, *256*, 2118–2121.
 (25) Palaniappan, V.; Terner, J. *J. Biol. Chem.*, in press.

so that direct comparison of the spectra is not possible. Band ν_2 might be more reliably identified by reconstituting HRP with mesoporphyrin in which the peripheral vinyl groups are replaced with ethyl groups and the ν_2 region is simplified.²⁶ It has been argued that the similar methyl ¹H NMR contact shifts for mesohemin- and native-HRP indicate that they have the same ground state and that the small downfield methine bridge proton contact shift observed for mesohemin-HRP is consistent with an a_{1u} ground-state assignment.²⁷

Whatever the situation turns out to be for HRP, the cytochrome P₄₅₀ compound I-like intermediate²⁸ is very likely to involve an a_{2u} radical. This is because the sixth ligand is the thiolate group of a cysteine residue.²⁹ Thiolate is a strong donor ligand, as is evident from the marked lowering of the Fe–C stretch of cytochrome P₄₅₀ CO adducts relative to imidazole–heme CO adducts³⁰

and also the anomalously low ν_4 porphyrin frequency in the reduced enzyme.³¹ Porphyrin mode ν_4 is composed of mainly pyrrole ring C _{α} –N and C _{α} –C _{β} stretching³² and is sensitive to the central metal oxidation state and the axial ligand electron donation.³³ Thiolate is even more likely than imidazole to push the a_{2u} orbital above the a_{1u} (although the electronic structure calculations have not shown the stronger thiolate donor effect^{20a,21}). Consequently, the Fe–O bond in the P₄₅₀ intermediate should be weakened by two effects, the direct influence of the trans-ligand electron donation^{12,34} and the porphyrin radical character. Both are expected to play important roles in the oxygen-transfer chemistry of the enzyme.

Acknowledgment. This work was supported by Grant DE-AC02-81-ER-10861 from the U.S. Department of Energy (T.G.S.). We thank Professor James Turner (Virginia Commonwealth University) for communicating results prior to publication.

- (26) Verna, A. L.; Mendelsohn, R.; Bernstein, H. *J. Chem. Phys.* **1974**, *61*, 383–387.
- (27) LaMar, G. N.; Thanabal, V.; Johnson, R. D.; Smith, K. M.; Parish, D. W. *J. Biol. Chem.* **1989**, *264*, 5428–5434.
- (28) Groves, J. T.; Haushalter, R. C.; Nakamura, M.; Nemo, T. E.; Evans, B. *J. Am. Chem. Soc.* **1981**, *103*, 2884–2886.
- (29) (a) Poulos, T. L.; Finzel, B. C.; Howard, A. J. *Biochemistry* **1986**, *25*, 5314–5322. (b) Champion, P. M.; Stallard, B. R.; Wagner, G. C.; Gunsalus, I. C. *J. Am. Chem. Soc.* **1982**, *104*, 5469–5472. (c) Dawson, J. H.; Holm, R. H.; Trudell, J. R.; Barth, G.; Linder, R. E.; Bunnenberg, E.; Djerassi, C. *J. Am. Chem. Soc.* **1976**, *98*, 3707–3709. (d) Stern, J. O.; Peisach, J. *J. Biol. Chem.* **1974**, *249*, 7495–7480.
- (30) (a) Li, X. Y.; Spiro, T. G. *J. Am. Chem. Soc.* **1988**, *110*, 6033–6046. (b) Champion, P. M. In *Biological Applications of Raman Spectroscopy*; Spiro, T. G., Ed.; John Wiley & Sons: New York, 1988; Vol. 3, Chapter 6. (c) Tsubaki, M.; Ichikawa, Y. *Biochemistry* **1986**, *25*, 3563–3570.

- (31) (a) Anzenbacher, P.; Evangelista-Kirkup, R.; Spiro, T. G. *Inorg. Chem.* **1989**, *28*, 4491–4495. (b) Ozaki, Y.; Kitagawa, T.; Kyogoku, Y.; Shimada, H.; Iizuka, T.; Ishimura, Y. *J. Biochem. (Tokyo)* **1976**, *80*, 1447–1451. (c) Champion, P. M.; Remba, R. D.; Chiang, R.; Fitchen, D. B.; Hager, L. P. *Biochem. Biophys. Acta* **1976**, *446*, 486–490.
- (32) (a) Li, X. Y.; Czernuszewicz, R. S.; Kincaid, J. R.; Su, Y. O.; Spiro, T. G. *J. Phys. Chem.* **1990**, *94*, 31–47. (b) Li, X. Y.; Czernuszewicz, R. S.; Kincaid, J. R.; Stein, P.; Spiro, T. G. *J. Phys. Chem.* **1990**, *94*, 47–61.
- (33) Spiro, T. G. In *Biological Applications of Raman Spectroscopy*; Spiro, T. G., Ed.; John Wiley & Sons: New York, 1988; Vol. 3, Chapter 1.
- (34) (a) Gaul, E. M.; Kassner, R. J. *Inorg. Chem.* **1986**, *25*, 3734–3740. (b) Buchler, J. W.; Kokisch, W.; Smith, P. D. In *Structure and Bonding*; Springer-Verlag: Berlin, 1978; Vol. 34, 79–134.